Analytical Biochemistry 620 (2021) 114138

Contents lists available at ScienceDirect

Analytical Biochemistry

journal homepage: www.elsevier.com/locate/yabio

Ultrasensitive and selective fluorescent sensor for cysteine and application to drug analysis and bioimaging

Luping Hu [a], Tao Zheng [b,**], Yanxi Song [c], Ji Fan [a], Hongqi Li [a,*], Ruiqing Zhang [a], Yi Sun [b]

[a] Key Laboratory of Science and Technology of Eco-Textiles, Ministry of Education, College of Chemistry, Chemical Engineering & Biotechnology, Donghua University, 2999 North Renmin Road, Shanghai, 201620, PR China
[b] Department of Health Technology, Technical University of Denmark, Kgs, Lyngby, 2800, Denmark
[c] College of Environmental Science and Engineering, Donghua University, 2999 North Renmin Road, Shanghai, 201620, PR China

ARTICLE INFO

Keywords:
Fluorescent sensor
Coumarin
Cysteine
Maleimide
Bioimaging
Drug analysis

ABSTRACT

A fluorescent sensor based on coumarin-maleimide conjugate was developed for efficient discrimination of Cys from Hcy and GSH in both organic and aqueous solution. Addition of Cys to the non-fluorescent sensor solution in DMF induced bright blue fluorescence and enhanced the fluorescence intensity by 320-fold while other amino acids and biothiols (Gly, Hcy, GSH, Glu, Val, Tyr, Arg, Trp, Lys, His, Leu, Phe, Asp and Met) did not bring about remarked change. The sensor responds to Cys extremely rapidly. If Cys was added to the sensor solution, the fluorescence intensity increased by 170-fold immediately and attained the maximum value in 5 min. A linear relationship was observed between Cys concentration within 2–20 μM and the fluorescence intensity of the sensor solution. The detection limit of the sensor toward Cys is as low as 4.7 nM. The sensor is also effective for specific detection of Cys in aqueous (DMF/H_2O = 9:1, v/v) solution. Practical application of the sensor to drug analysis and bioimaging of living Hela cells has been verified. Possible sensing mechanism of the sensor toward Cys has been proposed.

1. Introduction

As the main representatives of biologically significant thiols, homocysteine (Hcy), cysteine (Cys) and γ-Lglutamyl-L-cysteinylglycine (glutathione, GSH) exert various important effects on human health [1,2]. Cys plays a vital role in regulation of protein function [3]. On the other hand, Cys exhibits neurotoxicity [4] and may induce senescence and decelerate cell growth in melanoma [5]. Thus efficient methods for detection of biothiols with both high sensitivity and selectivity and for specific sensing of Cys over other biothiols are in urgent demand. As one of the best choices for biothiols detection, fluorescent sensors derived from different fluorophore platforms receive extensive attention and application in view of their short response time, low detection limit, and high sensitivity and selectivity [6–16]. Considering that the sulfhydryl group in biothiol molecules is strongly nucleophilic and shows strong binding affinity to mercury and copper ions, several strategies for reasonable design of biothiol sensors have been developed including Michael addition [17–21], cyclization reaction with cyano group [22] or aldehyde [23,24], conjugate addition to an acrylate followed by subsequent cyclization reaction [25–33], sulfonamide [34,35] or sulfonate esters cleavage [36–38], S–S bond [39,40] or Se–N bond cleavage [41,42], nucleophilic substitution [43–45], metal complex-displacement coordination [46–48], and indicator displacement [49,50]. As a typical and excellent Michael acceptor, maleimide group can be attached to various fluorophores to construct fluorescent sensors for specific sensing of thiols. Following the pioneering work reported by Sippel [51,52], fluorogenic chemosensors based on different fluorophores functionalized with maleimide were designed and synthesized on the purpose of biothiol sensing [53–60]. It is found that most of these sensors are efficient for detecting Cys, Hcy and GSH simultaneously, only a small part of them can be utilized for discriminating Cys from Hcy and GSH. Specific detection of Cys by using the fluorescent chemosensors is limited due to the drawbacks including the introduction of heavy metal ions, complicated synthetic procedures and a relatively long response time from 10 min to 60 min. Development of ultrasensitive fluorogenic chemosensors to distinguish Cys from other biothiols is in high demand and remains to be a huge challenge as a result of the similar structures and comparable reactivities between Cys and other

* Corresponding author.
** Corresponding author.
E-mail address: hongqili@dhu.edu.cn (H. Li).

https://doi.org/10.1016/j.ab.2021.114138
Received 24 November 2020; Received in revised form 29 January 2021; Accepted 12 February 2021
Available online 24 February 2021

biothiols. With it in mind that maleimide-based fluorogenic sensors respond to biothiols very rapidly [54,56] and following the efforts in construction of highly selective fluorescent biothiol chemosensors in our group [46,61], we developed a new structurally simple yet ultrasensitive and selective fluorometric chemosensor for efficiently discriminating Cys from Hcy and GSH by taking advantage of the easy response between thiols and maleimide which is incorporated into coumarin, the excellent fluorophore for construction of fluorescent sensors [62,63]. In this paper we report the design, synthesis, structural characterization, responsive performance, and application in drug analysis and bioimaging of the coumarin-maleimide dyad-based specific chemosensor for Cys.

2. Experimental part

2.1. Chemicals and measurements

The chemicals and solvents for synthesis were analytically pure and were used as received unless otherwise stated. The drug Super-Bio L-CYSTEINE was produced in Hubei Shubang Pharmaceutical Co., Ltd. An WRS-2A melting apparatus was utilized to determine melting points. An Bruker ACF-500 spectrometer was used for recording ^{1}H NMR and ^{13}C NMR spectra with.CD_3Cl and Me_4Si as solvent and the internal reference, respectively. FT-IR spectra were recorded on an Bruker Tensor 27 spectrophotometer. An Agilent 1100 Series LC/MSD Trap mass spectrometer was used for mass spectra recording by using electronspray ionization (ESI). An 7600CRT spectrophotometer and an FS5 spectrofluorometer were utilized for measuring UV–vis absorption spectra and fluorescence spectra, respectively.

2.2. Synthesis of ethyl 6-nitro-2-oxo-2H-chromene-3-carboxylate (compound 1)

Diethyl malonate (4.40 g, 27.5 mmol) and 5-nitrosalicylaldehyde (4.19 g, 25 mmol) were added to a flask and then dissolved in anhydrous ethanol (50 mL), followed by addition of catalytic amount of piperidine. The solution was stirred and refluxed for 2 h. After the reaction had finished the solution was cooled to ambient temperature and the resulted yellow powder was filtered out. Recrystallization of the crude product with ethanol as solvent gave compound **1** (6.0 g, 90%) as yellowish solid with m.p. 202–204 °C (literature value: 203–204 °C [64]).

2.3. Synthesis of ethyl 6-amino-2-oxo-2H-chromene-3-carboxylate (compound 2)

Compound **1** (2.63 g, 10 mmol) and stannous chloride (9.5 g, 50 mmol) were added to a flask. Dry ethanol (30 mL) was used to dissolve the mixture. The resulted solution was refluxed and stirred for 1 h. After the reaction had finished, the solution was evaporated under reduced pressure to remove the solvent. Ethyl acetate (300 mL) was used to dissolve the residue. $NaHCO_3$ solution (400 mL) was added for washing. Then the solution was dried over anhydrous $MgSO_4$. After filtration the solution was evaporated for crystallization. The solid was collected and was recrystallized from EtOH to give compound **2** (1.5 g, 64%) as reddish brown powder with m.p. 179–181 °C (literature value: 180–182 °C [64]).

2.4. Synthesis of N-(3-ethoxycarbonyl-2-oxo-2H-chromen-6-yl) maleimide (A1)

Compound **2** (223 mg, 1 mmol), glacial acetic acid (10 mL) and maleic anhydride (108 mg, 1.1 mmol) were added to a flask. The mixture was stirred then the solution was refluxed for 6 h. After reaction the mixture was cooled to ambient temperature. Evaporation under reduced pressure to remove solvent yielded light yellow solid, which was submitted to column chromatography for purification. Petroleum ether/ethyl acetate (1:1, v/v) was used as eluent to produce sensor **A1** (0.17 g, 53%) as light yellow powder with m.p. 178–180 °C. IR (KBr pellet): ν = 3085, 3045, 2966, 1747, 1708, 1569, 1489, 1430, 1371, 1222, 1133, 1024, 865, 816 cm^{-1}. ^{1}H NMR (400 MHz, $CDCl_3$) δ 8.45 (s, 1H), 7.65–7.61 (m, 2H), 7.38 (d, J = 9.6 Hz, 1H), 6.85 (s, 2H), 4.35 (q, J = 7.1 Hz, 2H), 1.34 (t, J = 7.1 Hz, 3H). ^{13}C NMR (101 MHz, $CDCl_3$) δ 167.91 (C═O), 161.64 (C═O), 155.14 (C═O), 152.77 (Ph–C), 146.74 (=C), 133.42 (=C), 130.27 (=C), 127.01 (Ph–C), 125.01 (Ph–C), 118.16 (Ph–C), 117.11 (Ph–C), 116.62 (Ph–C), 61.12 (CH_2), 13.19 (CH_3). ESI-

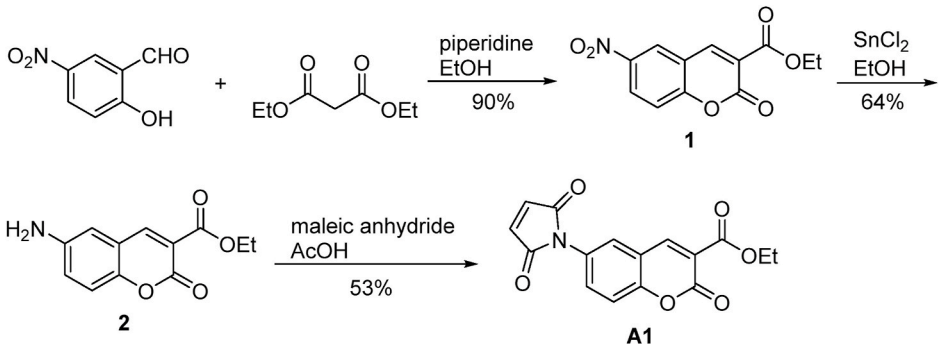

Scheme 1. Synthetic route to sensor **A1**.

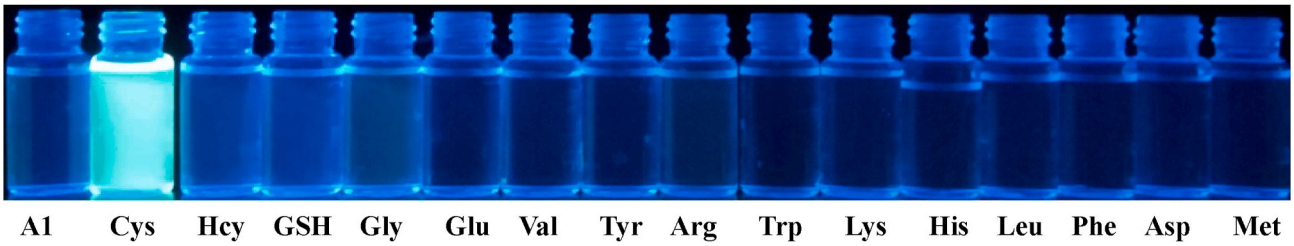

Fig. 1. Color of sensor **A1** solution (20 μM in DMF) before and after addition of 1.0 equivalent of Cys, Hcy, GSH, Gly, Glu, Val, Tyr, Arg, Trp, Lys, His, Leu, Phe, Asp or Met under UV irradiation. (For interpretation of the references to colour in this figure legend, the reader is referred to the Web version of this article.)

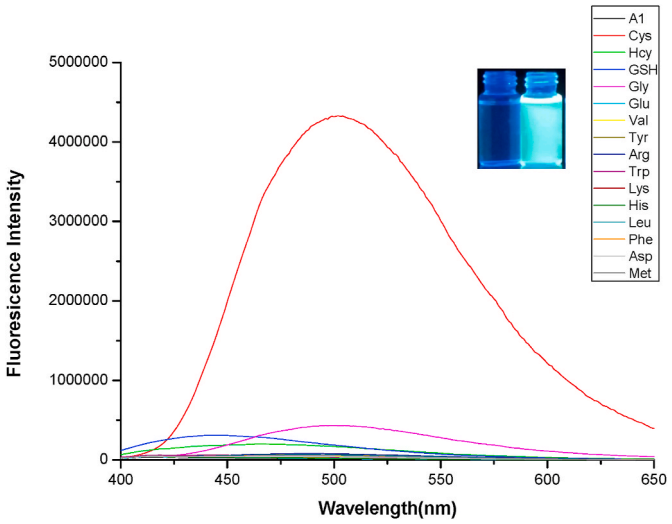

Fig. 2. Fluorescence emission spectra of sensor **A1** (20 μM) before and after addition of 20 μM of Cys, Hcy, GSH, Gly, Glu, Val, Tyr, Arg, Trp, Lys, His, Leu, Phe, Asp or Met in DMF with λ_{ex} of 369 nm.

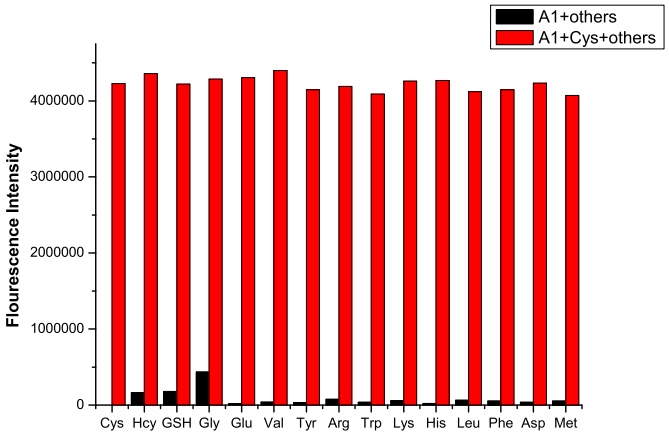

Fig. 3. Fluorescence intensity at 502 nm of **A1** (20 μM) upon addition of 20 μM of Hcy, GSH, Gly, Glu, Val, Tyr, Arg, Trp, Lys, His, Leu, Phe, Asp or Met without (black bars) or with Cys (red bars) in DMF. (For interpretation of the references to colour in this figure legend, the reader is referred to the Web version of this article.)

MS: *m/z* 313 (M^+).

2.5. Measurements of the absorption and fluorescence emission spectra

UV–vis and fluorescence spectra were determined in *N*,*N*-dimethylformamide (DMF) or DMF/H_2O (9:1, v/v) at ambient temperature by using sensor **A1** solution of 20 μM concentration. The excitation wavelength was 369 nm with both the excitation and emission slit width being 10 nm in all the fluorescence titration experiments. The analytes were added to a cuvette of 2 mL volume by a microliter syringe.

2.6. Preparation of drug samples for determination

One pill of the drug Super-Bio L-CYSTEINE (18%) containing 0.400 g drug powder and 72 mg (0.595 mmol) of the effective constituent Cys was dissolved in ultrapure water (297.5 mL) to obtain the drug sample solution (Cys concentration 2 mM). Then 25 μL, 50 μL or 75 μL of the above solution was measured with a pipette and was diluted 10 times to obtain the drug samples with a concentration of 5 μM, 10 μM or 15 μM, respectively.

2.7. Cell imaging

Hela cells were supplied by the American Type Culture Collection. Storage of all the cells was achieved in a 100% humidity atmosphere of 37 °C and 5% CO_2. Firstly, Hela cells were cultured in the flasks, supplemented with DMEM, 10% fetal bovine serum and 1% antibiotics in a 100% humidity atmosphere of 37 °C and 5% CO_2. Then sensor **A1** (20 μM in DMSO) was incubated with Hela cells for 30 min at 37 °C as well as washed with phosphate-buffered saline three times after incubation. In control group, Hela cells were incubated with *N*-ethylmaleimide (0.1 mM) for 30 min at 37 °C. Next, the incubation solution was washed with phosphate-buffered saline (2 mL × 3) to remove the excess *N*-ethylmaleimide. Sensor **A1** (20 μM in DMSO) was incubated with above *N*-ethylmaleimide pre-treated Hela cells for 30 min at 37 °C and washed with phosphate-buffered saline three times soon after before the cell imaging.

3. Results and discussion

3.1. Preparation of sensor *A1*

The designed sensor **A1** was synthesized by utilizing a three-step protocol and the synthetic route was illustrated in Scheme 1. Compound **1** was prepared from the raw materials diethyl malonate and 5-nitrosalicylaldehyde in 90% yield by Knoevenagel condensation

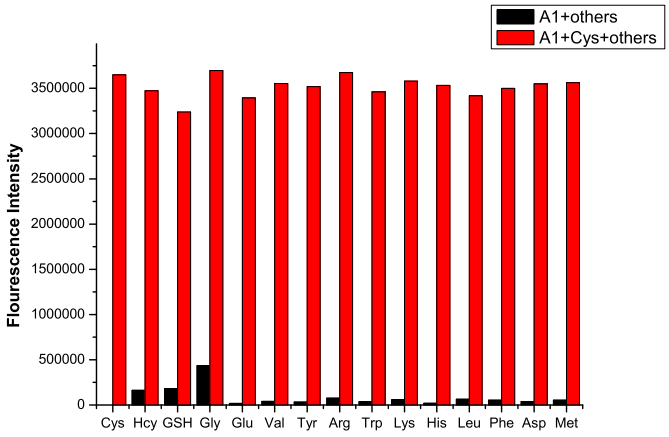

Fig. 4. Fluorescence intensity at 502 nm of **A1** (20 μM) upon addition of 100 μM of Hcy, GSH, Gly, Glu, Val, Tyr, Arg, Trp, Lys, His, Leu, Phe, Asp or Met without (black bars) or with Cys (red bars) in DMF. (For interpretation of the references to colour in this figure legend, the reader is referred to the Web version of this article.)

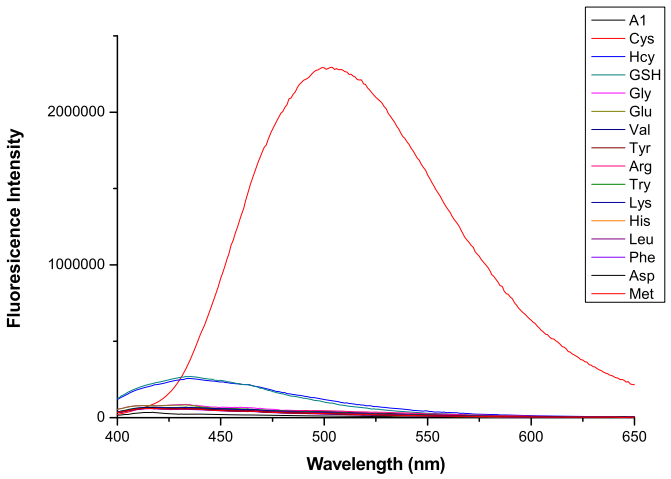

Fig. 5. Fluorescence emission spectra of sensor **A1** (20 μM) obtained immediately after addition of 20 μM of Cys, Hcy, GSH, Gly, Glu, Val, Tyr, Arg, Trp, Lys, His, Leu, Phe, Asp or Met in DMF with λ_{ex} being 369 nm.

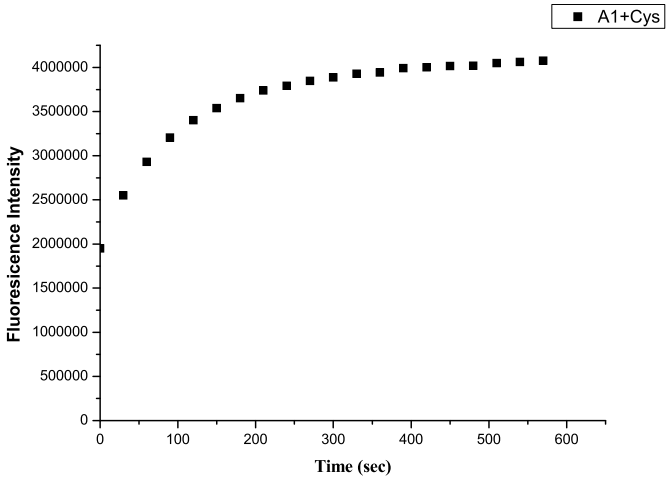

Fig. 6. Changes in the fluorescence intensity at 502 nm of **A1** (20 μM) upon addition of 1 equivalent of Cys in DMF with time (λ_{ex} = 369 nm).

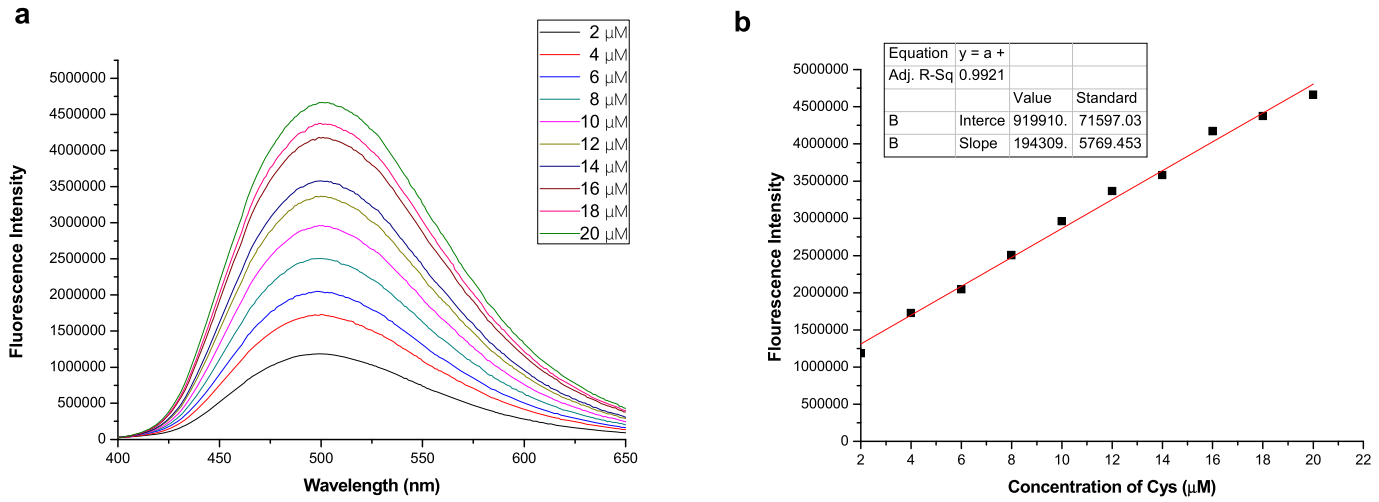

Fig. 7. (a) Fluorescence spectra of **A1** (20 μM) upon addition of different concentration of Cys (2–20 μM) in DMF. (b) Linear relationship between the fluorescence intensity at 502 nm of **A1** (20 μM) and Cys concentration (0–20 μM) in DMF.

reaction. Piperidine and ethanol were used as the catalyst and solvent, respectively. Reduction of compound **1** with stannous chloride in ethanol gave compound **2** in 64% yield. Imidation reaction between compound **2** and maleic anhydride afforded sensor **A1** in 53% yield. This condensation-reduction-imidation protocol is efficient for convenient and straightforward synthesis of divergent coumarin-based chemosensors substituted with maleimide at different position since various nitrosalicylaldehydes are available. The chemical structure of the sensor was characterized by IR spectrum (Fig. S1), ^{1}H NMR (Fig. S2), ^{13}C NMR (Fig. S3) and MS (Fig. S4).

3.2. Sensing behavior of *A1* in DMF

Sensor **A1** shows bad solubility in water but can be dissolved readily by organic solvent DMF and acetonitrile. Considering that sensor **A1** exhibits the strongest absorption and fluorescence emission in DMF, sensing performance of **A1** was investigated in two media: DMF and DMF/H_2O (9:1, v/v).

The absorption spectra of sensor **A1** (20 μM solution in DMF) were measured before and after addition of different amino acids including Arg, Asp, Cys, Glu, Gly, GSH, Hcy, His, Leu, Lys, Met, Phe, Trp, Tyr, and Val (20 μM) (Fig. S5). No obvious spectral change was observed after addition of the amino acids. If the solution of sensor **A1** or **A1**/amino acid (20 μM in DMF) was irradiated with a UV lamp (λ = 365 nm), it could be observed that sensor **A1** displayed extremely weak fluorescence and the solution containing sensor **A1** and Cys presented strong bright blue fluorescence. The fluorescence did not change markedly upon addition of other amino acids as showed in Fig. 1. Thus **A1** can be utilized for visual distinguishing of Cys from Hcy, GSH and other amino acids under UV irradiation.

Fluorescence spectra of sensor **A1** (20 μM solution in DMF) were measured before and after addition of 20 μM of Arg, Asp, Cys, Glu, Gly, GSH, Hcy, His, Leu, Lys, Met, Phe, Trp, Tyr, and Val as showed in Fig. 2. It was visible that a broad emission band appeared at around 502 nm after addition of Cys. This means that a red shift of 87 nm compared to **A1** has been induced by addition of Cys with 320-fold enhancement of the fluorescence intensity. Addition of other amino acids including Gly and biothiols Hcy and GSH also caused enhancement of the fluorescence but the intensities were quite small compared with that of Cys. It can be considered that the addition of amino acids other than Cys induce negligible changes in the fluorescence emission spectra of **A1**. The results demonstrate the high selectivity of sensor **A1** toward Cys over other common competitive amino acids and biothiols including Hcy, GSH, Gly, Glu, Val, Tyr, Arg, Trp, Lys, His, Leu, Phe, Asp and Met.

The competitive experiments were conducted in the presence of Cys over other amino acids. Fluorescence intensity at 502 nm of **A1** (20 μM) upon addition of Arg, Asp, Hcy, His, Glu, Gly, GSH, Leu, Lys, Met, Phe, Trp, Tyr or Val without or with Cys (20 μM in DMF) were recorded in Fig. 3. The fluorescence intensity of **A1** with Cys was not influenced substantially by the addition of competitive amino acids including Hcy, GSH and Gly. To further demonstrate the excellent anti-interference feature of sensor **A1**, fluorescence intensity at 502 nm of **A1** (20 μM) upon addition of 5 equivalent (100 μM) of Hcy, GSH, Gly, Glu, Val, Tyr, Arg, Trp, Lys, His, Leu, Phe, Asp or Met without or with 1 equivalent of Cys in DMF were measured and showed in Fig. 4. Though the addition of a large amount of competitive amino acids especially GSH brought about the fluorescence intensity decrease of **A1** with Cys, the changes were small and could not influence substantially the fluorescence turn-on detection of Cys by **A1**. This means the fluorescent sensor **A1** exhibits excellent selectivity and anti-interference ability. Therefore sensor **A1** is applicable for highly selective fluorogenic discrimination of Cys from other common amino acids and biothiols.

Response time of sensor **A1** toward Cys was investigated. Fluorescence of sensor **A1** solution (20 μM in DMF) measured immediately after addition of Arg, Asp, Cys, Glu, Gly, GSH, Hcy, His, Leu, Lys, Met, Phe, Trp, Tyr or Val (20 μM) excited at a wavelength of 369 nm were showed in Fig. 5. It is apparent that sensor **A1** responds to Cys very rapidly and adding Cys to sensor **A1** solution induces the fluorescence intensity enhancement by 170-fold instantly. Then the time-dependency of the fluorescence emission of sensor **A1** (20 μM in DMF) at 502 nm after adding Cys (1 equivalent) excited at 369 nm was investigated. Changes in the fluorescence emission intensity at 502 nm of sensor **A1** upon addition of 1 equivalent of Cys with time were recorded and showed in Fig. 6. The results revealed clearly that after Cys had just been added, the fluorescence intensity increased immediately to a high point. When the

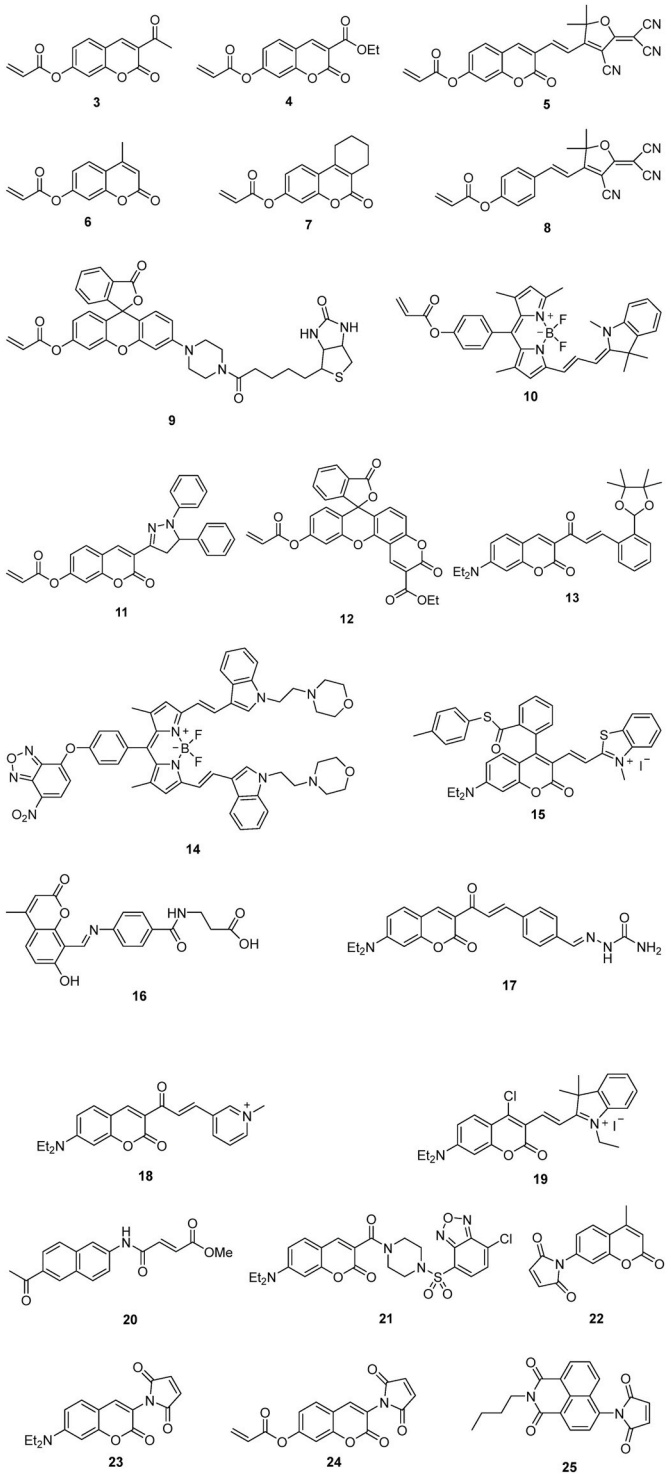

Scheme 2. Structures of reported fluorescent sensors for specific detection of Cys.

Table 1
Performance comparison of typical fluorescent sensors for specific detection of Cys.

Sensor	Limit of detection	Response time	Reference
3	0.657 μM	40 min	[25]
4	60 nM	10 min	[66]
5	0.2 μM	10 min	[29]
6	47.7 nM	30 min	[30]
7	70 nM	20 min	[67]
8	40 nM	12 min	[33]
9	0.307 μM	40 min	[32]
10	50 nM	4 min	[28]
11	5.08 μM	40 min	[26]
12	84 nM	5 min	[27]
13	14 μM	10 min	[18]
14	22 nM	30 min	[68]
15	60 nM	30 min	[69]
16	0.15 μM	3 min	[70]
17	11.1 nM	3 min	[17]
18	25 nM	1 min	[71]
19	46.3 μM	30 min	[72]
20	0.48 μM	15 min	[21]
21	1.4 μM	60 min	[39]
22	38 nM	4 s	[53]
23	14 nM	20 min	[57]
24	13.7 nM	35 min	[73]
25	4.8 nM	10 min	[54]
25	2.0 nM	10 min	[56]
A1	4.7 nM	5 min	This work

time of the reaction between Cys and sensor **A1** was prolonged, the fluorescence intensity increased gradually and much slowly and leveled off to a saturation value in 5 min. It is concluded that sensor **A1** exhibits extremely rapid response to Cys.

Titration experiments of Cys were performed to investigate the sensitivity of sensor **A1**. The fluorescence emission of sensor **A1** solution (20 μM in DMF) after adding different concentration (2–20 μM) of Cys was showed in Fig. 7a. And the concentration-dependent responses of sensor **A1** to Cys in DMF were showed in Fig. 7b. With the increment of Cys concentration, the fluorescence intensity at 502 nm increased gradually. The fluorescence intensity is linearly proportional to the concentration of added Cys and the linear fitting equation can be depicted as $Y = 919911 + 194309X$ with $R^2 = 0.9921$. The limit of detection (LOD) of **A1** for Cys was found to be 4.7 nM, based on the definition $L = 3S/K$ of IUPAC, where L is the detection limit, S denotes the standard deviation of fluorescence intensity of blank, and K is slope of the calibration curve [65].

To compare the sensing performance of sensor **A1** with other reported examples, chemical structures of typical fluorescent sensors for specific detection of Cys have been outlined in Scheme 2.

Among the various fluorogenic Cys sensors, the fluorophore mainly concentrates on coumarin, naphthalimide, rhodamine, BODIPY, and naphthalene. The sensing mechanisms include Michael addition, conjugate addition–cyclization reaction with an acrylate, and cleavage of sulfonamide. Acrylate and maleimide groups, as typical Michael acceptors, exhibit superior features and contribute heavily to construction of highly sensitive fluorescent chemosensors for specific detection of

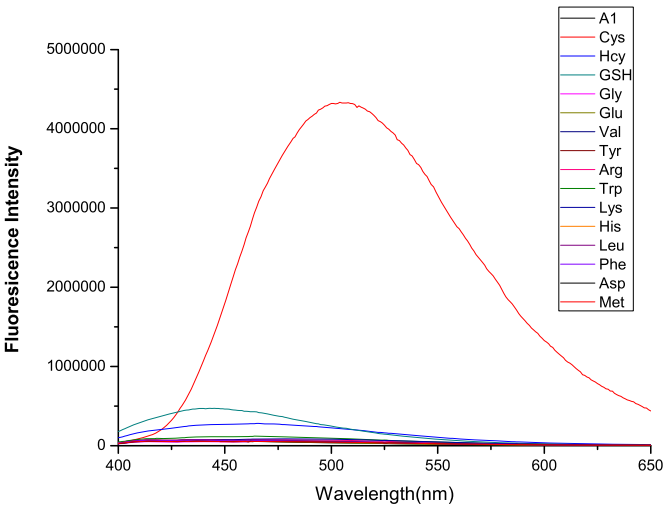

Fig. 9. Fluorescence emission spectra of sensor **A1** (20 μM) before and after addition of 20 μM of Cys, Hcy, GSH, Gly, Glu, Val, Tyr, Arg, Trp, Lys, His, Leu, Phe, Asp or Met in DMF/H_2O (9:1, v/v) with λ_{ex} of 369 nm.

Cys. Performance comparison of typical fluorescent sensors for specific detection of Cys was summarized in Table 1. Several points are noteworthy from the data in the table. LOD values of the sensors range from 2.0 nM to 0.657 μM while the response time is in the range of 4 sec–60 min. Coumarin serves a favorable fluorophore for construction of ultrasensitive fluorescent Cys sensors with short response time (e.g. sensor **12**, **16**–**18**, **22** and **A1**). The acrylate group is the most widely employed reaction functionality for Cys due to its high reactivity and specificity. Sensors based on the acrylate recognition site (sensor **3**–**12**) show LOD from 40 nM to 0.657 μM, inferior to the maleimide-based counterparts (sensor **22**–**25** and **A1**) which exhibit low LOD values of 2.0–38 nM. Sensor **A1** is undoubtedly among the best in respect of its low LOD (4.7 nM), rapid response (several sec–5 min), extraordinary fluorescence enhancement (320-fold), and facile synthesis.

3.3. *Sensing behavior of **A1** in DMF/H_2O (9:1, v/v)*

No substantial UV–vis spectral change was observed after addition of amino acids including Arg, Asp, Cys, Glu, Gly, GSH, Hcy, His, Leu, Lys, Met, Phe, Trp, Tyr and Val (20 μM) to sensor **A1** solution (20 μM) in DMF/H_2O (9:1, v/v) (Fig. S6). Solution of sensor **A1** (20 μM) in DMF/H_2O (9:1, v/v) is non-fluorescent and upon addition of Cys (20 μM) strong bright blue fluorescence was visible under UV irradiation (λ = 365 nm). Adding other amino acids or biothiols (Arg, Asp, Glu, Gly, GSH, Hcy, His, Leu, Lys, Met, Phe, Trp, Tyr and Val) failed to cause distinct change in the fluorescence, as showed in Fig. 8. Thus **A1** can be utilized for visual discriminating Cys from Hcy, GSH and other amino acids under UV irradiation in a partially aqueous solution.

Changes in the fluorescence (excited at 369 nm) of sensor **A1** solution (20 μM) caused by addition of amino acids Arg, Asp, Cys, Glu, Gly,

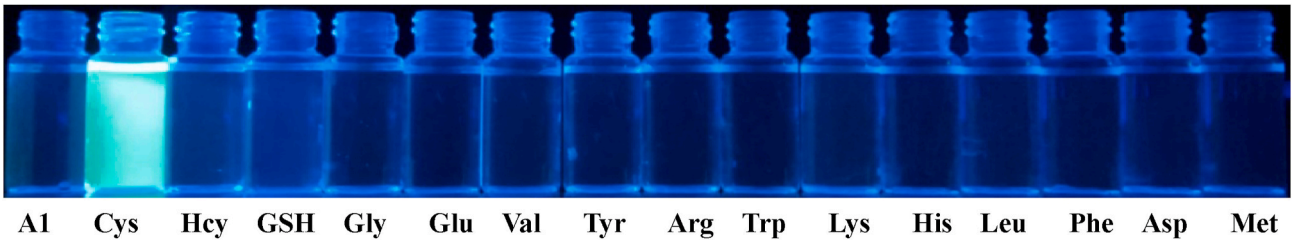

Fig. 8. Color of sensor **A1** solution (20 μM) in DMF/H_2O (9:1, v/v) before and after addition of 1 equivalent of Cys, Hcy, GSH, Gly, Glu, Val, Tyr, Arg, Trp, Lys, His, Leu, Phe, Asp or Met under UV irradiation. (For interpretation of the references to colour in this figure legend, the reader is referred to the Web version of this article.)

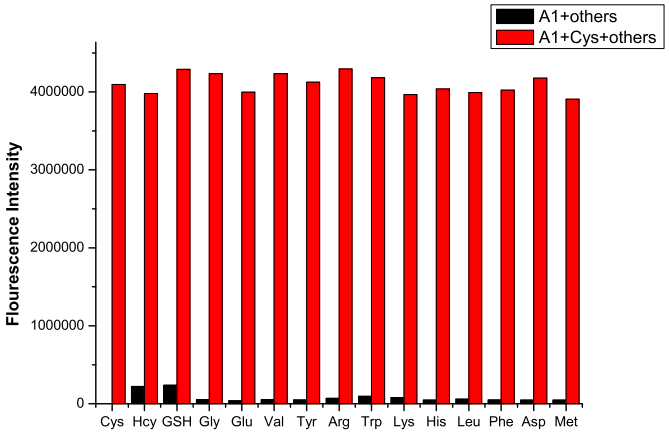

Fig. 10. Fluorescence intensity at 502 nm of **A1** (20 μM) upon addition of 20 μM of Hcy, GSH, Gly, Glu, Val, Tyr, Arg, Trp, Lys, His, Leu, Phe, Asp or Met without (black bars) or with Cys (red bars) in DMF/H_2O (9:1, v/v). (For interpretation of the references to colour in this figure legend, the reader is referred to the Web version of this article.)

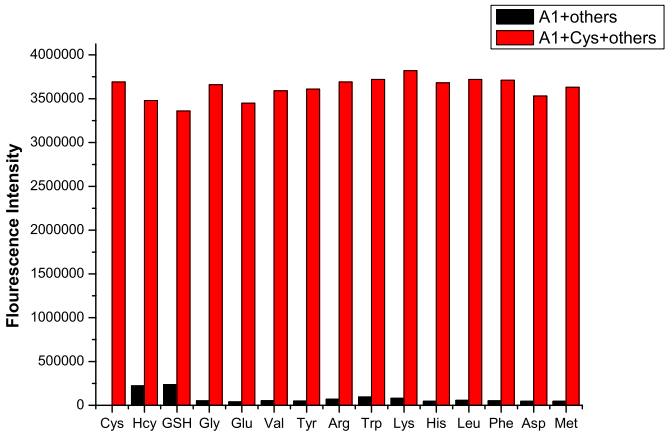

Fig. 11. Fluorescence intensity at 502 nm of **A1** (20 μM) upon addition of 100 μM of Hcy, GSH, Gly, Glu, Val, Tyr, Arg, Trp, Lys, His, Leu, Phe, Asp or Met without (black bars) or with Cys (red bars) in DMF/H_2O (9:1, v/v). (For interpretation of the references to colour in this figure legend, the reader is referred to the Web version of this article.)

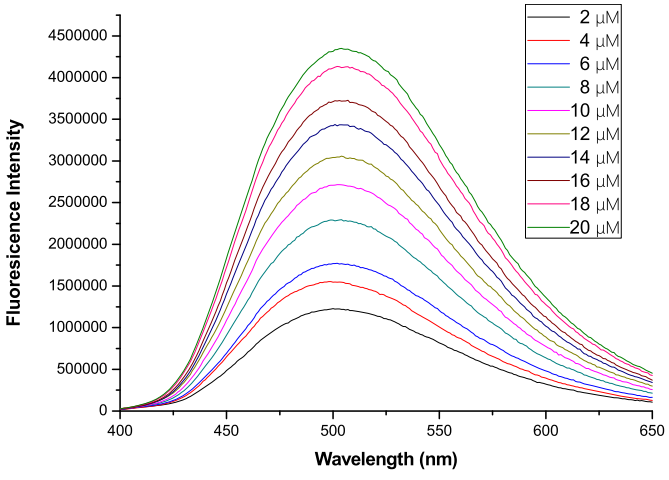

Fig. 12. Fluorescence response of **A1** (20 μM) with increasing amount of Cys (2–20 μM) in DMF/H_2O (9:1, v/v).

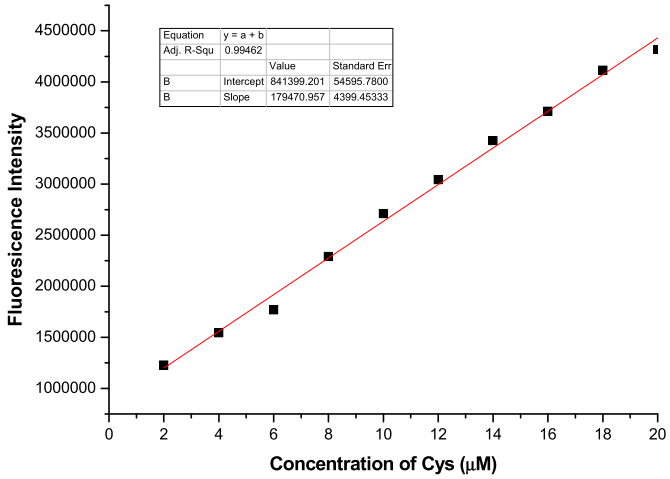

Fig. 13. Linear relationship between the fluorescence intensity at 502 nm and Cys concentration (2–20 μM) in DMF/H_2O (9:1, v/v).

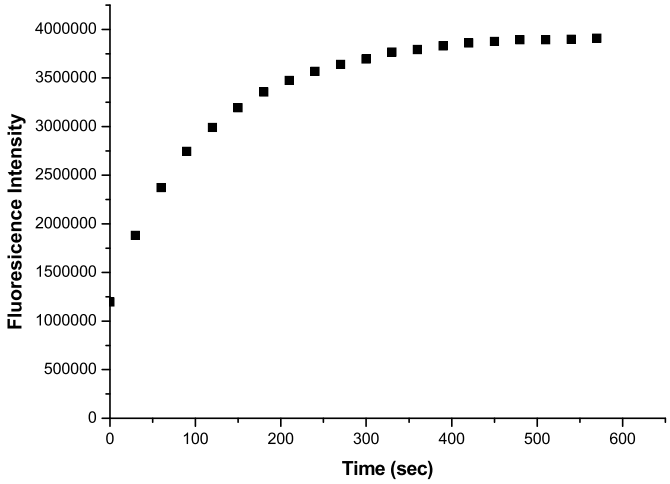

Fig. 14. Changes in the fluorescence intensity at 502 nm of **A1** (20 μM) upon addition of 1 equivalent of Cys in DMF/H_2O (9:1, v/v) with time (λ_{ex} = 369 nm).

GSH, Hcy, His, Leu, Lys, Met, Phe, Trp, Tyr or Val (20 μM) in DMF/H_2O (9:1, v/v) were determined as showed in Fig. 9. It was visible that a broad emission band appeared at around 502 nm upon adding Cys and the emission intensity was hugely enhanced. Negligible change in fluorescence emission at 502 nm was observed after addition of other amino acids including Hcy and GSH. The results demonstrate the high selectivity of sensor **A1** toward Cys over other common competitive amino acids and biothiols including Hcy, GSH, Gly, Glu, Val, Tyr, Arg, Trp, Lys, His, Leu, Phe, Asp and Met in a partially aqueous solution DMF/H_2O (9:1, v/v).

To investigate the anti-interference property of sensor **A1** for selective sensing Cys in an aqueous medium, competitive experiments were conducted in the presence of Cys over other amino acids. Fluorescence intensity at 502 nm of **A1** (20 μM) upon addition of 1 equivalent (20 μM) of Arg, Asp, Glu, Gly, GSH, Hcy, His, Leu, Lys, Met, Phe, Trp, Tyr or Val without or with Cys in DMF/H_2O (9:1, v/v) were measured as showed in Fig. 10. The fluorescence intensity of **A1** did not change substantially upon adding competitive analytes including Hcy, GSH and Gly. Furthermore, fluorescence intensity at 502 nm of **A1** (20 μM) upon addition of 5 equivalent (100 μM) of Hcy, GSH, Gly, Glu, Val, Tyr, Arg, Trp, Lys, His, Leu, Phe, Asp or Met without or with 1 equivalent of Cys in

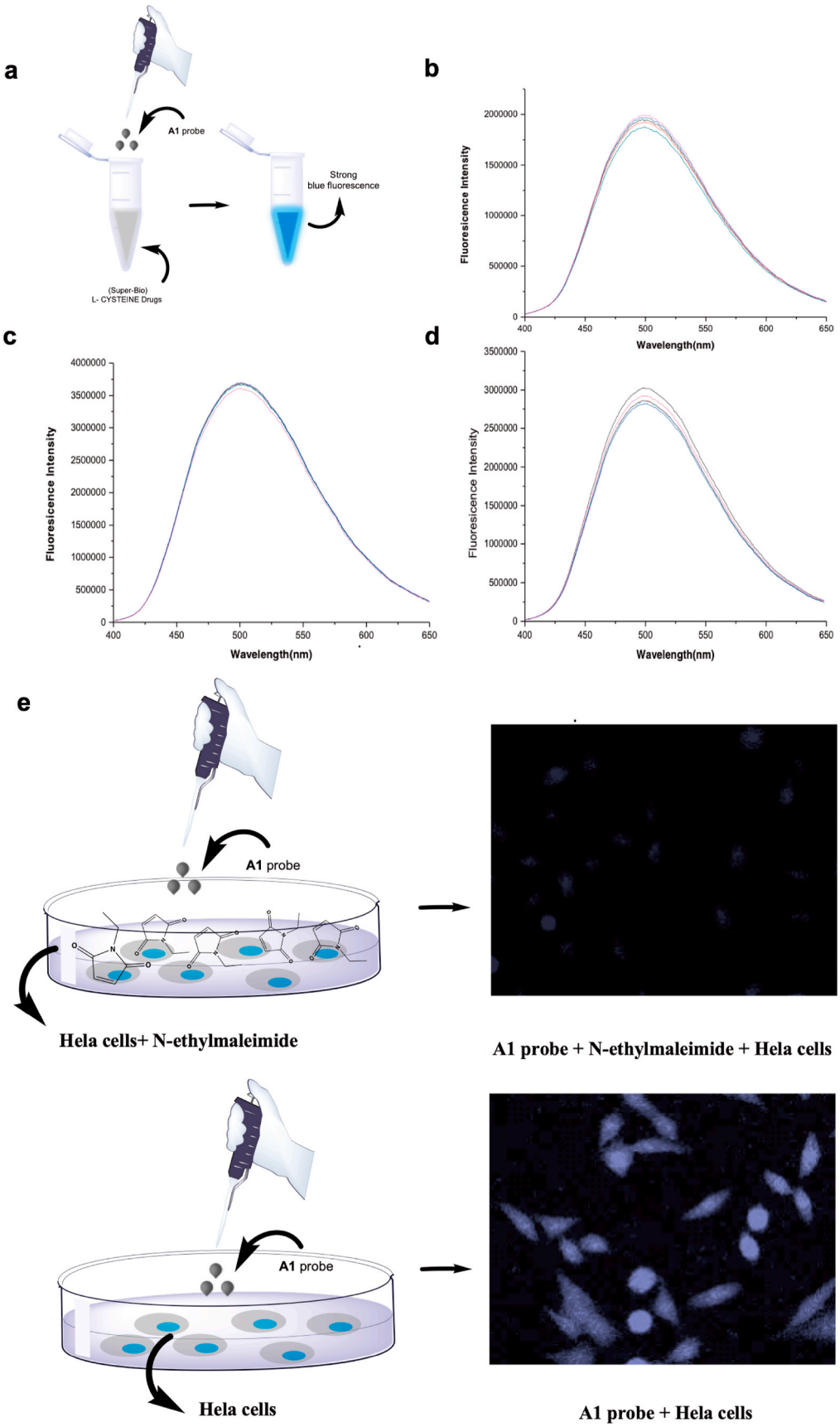

Fig. 15. (a) Schematic illustration of application of probe **A1** in drug analysis. Changes in fluorescence emission intensity at 502 nm (λ_{ex} = 369 nm) of probe **A1** (20 μM) upon addition of different concentrations of drug L-**CYSTEINE**. (b) 5 μM. (c) 10 μM. (d) 15 μM and (e) cell bioimaging with **A1** probe, fluorescence image at the blue channel. (For interpretation of the references to colour in this figure legend, the reader is referred to the Web version of this article.)

Table 2
Quantitative analytical results of Cys concentration in drug Super-Bio L-CYSTEINE by using sensor **A1**.

Added/ μM	Determined/μM					Average/ μM	RSD/ %
5	5.25	5.12	5.37	4.87	5.49	5.22	4.4
10	10.79	9.97	9.95	10.32	11.04	10.41	4.1
15	14.18	14.25	14.24	14.13	13.82	14.12	5.9

DMF/H_2O (9:1, v/v) were determined as showed in Fig. 11. Though the addition of a large amount of competitive amino acids brought about decrease in the fluorescence intensity, enhancement in the fluorescence emission of sensor **A1** by addition of Cys was still obvious and the fluorescence turn-on detection of Cys by **A1** was not influenced substantially. It can be concluded that sensor **A1** exhibits superior selectivity and anti-interference ability. Therefore **A1** may be applicable for highly selective fluorescence turn-on discriminating Cys from Hcy, GSH and other common amino acids in a partially aqueous solution.

For investigating the sensitivity and the detection limit of sensor **A1** for Cys in an aqueous medium, titration experiments of Cys were performed and the fluorescence spectra of **A1** (20 μM) in DMF/H_2O (9:1, v/v) upon addition of Cys with different concentration (2–20 μM) were determined (Fig. 12). The corresponding concentration-dependent responses of sensor **A1** to Cys in DMF/H_2O (9:1, v/v) were showed in Fig. 13. It is visible that the fluorescence intensity at 502 nm increased gradually with the increment of Cys concentration from 2 μM to 20 μM. The fluorescence intensity is linearly proportional to the concentration of added Cys and the linear fitting equation can be obtained as $Y = 841398 + 179471X$ with $R^2 = 0.9946$. The LOD of **A1** for Cys was calculated to be 14 nM.

Response time of sensor **A1** toward Cys in DMF/H_2O (9:1, v/v) was investigated. The time-dependency of the fluorescence intensity at 502 nm of **A1** (20 μM) upon addition of Cys (1 equivalent) in DMF/H_2O (9:1, v/v) was investigated. Changes in the fluorescence intensity at 502 nm of sensor **A1** (20 μM) in DMF/H_2O (9:1, v/v) upon addition of 1 equivalent of Cys with time were recorded and showed in Fig. 14. From the results it is found that upon addition of Cys the fluorescence intensity was enhanced sharply by ca. 180-fold in 1 min then the increase in the fluorescence intensity became slow. The fluorescence intensity approached to a saturation value in 7 min. The results reveal the rapid response of sensor **A1** to Cys in a partially aqueous medium.

3.4. Application of *A1* in drug analysis and bioimaging

It has been ascertained that the emission of sensor **A1** at 502 nm increased gradually with the increment of Cys concentration and the fluorescence intensity is linearly proportional to the concentration of added Cys within a range of 2–20 μM. Therefore the potential of probe A1 for quantitative analysis of Cys content in drugs containing Cys was explored. Changes in fluorescence emission intensity at 502 nm (λ_{ex} = 369 nm) of probe A1 (20 μM) upon addition of the drug Super-Bio L-CYSTEINE containing different concentrations of Cys (5 μM, 10 μM or 15 μM) were measured and showed in Fig. 15a,b,c,d. The analytical results are listed in Table 2. It can be seen that reliable data have been obtained and the relative standard deviation (RSD) of this fluorescence method is less than 6%. These test results demonstrate that the designed sensor **A1** is applicable for the quantitative analysis of Cys in real samples like drugs.

As mentioned above, the as-synthesized probe **A1** shows good applicability for quantitative analysis of Cys in drugs, which drives us to explore further potential utilization of **A1** probe in detecting Cys in living cells. The bioimaging experiments were conducted in living Hela cells under confocal fluorescence microscope. Firstly, Hela cells were cultured with **A1** probe at a concentration of 20 μM in DMSO. As showed in Fig. 15e, there is a stronger fluorescence signal which could be observed in the cells through the blue channel after 30 min incubation. However, in the control group, we selected a traditional thiol-blocking reagent called *N*-ethylmaleimide to pre-treat the cells. The probe **A1** (20 μM in DMSO) was incubated with *N*-ethylmaleimide (0.1 mM) pre-treated cells and no fluorescence signal could be observed after the treatment with **A1** probe (20 μM in DMSO) for 30 min, validating that **A1** probe is more sensitive to the endogenous Cys in living cells with satisfactory cell membrane penetration ability.

3.5. Sensing mechanism of *A1*

A reasonable sensing mechanism of sensor **A1** for fluorescence detection of Cys was proposed, as showed in Scheme 3. Sensor **A1** has a 3-ethoxycarbonyl-coumarin- 6-maleimide structure with the maleimide group as the specific reaction site for recognizing Cys. This maleimide group was linked directly to the coumarin skeleton and triggered an intramolecular charge transfer (ICT) effect. Sensor **A1** showed non-fluorescence due to a dual-quenching mechanism—ICT and an efficient photoinduced electron transfer (PET) quenching effect involving the Lowest Unoccupied Molecular Orbital (LUMO) of the maleimide moiety [56]. Upon Michael addition between Cys and the maleimide group, this orbital disappeared and the ICT process in the system was also switched off. Thus fluorescence emission of the system was recovered to generate a fluorescence turn-on response for sensor **A1** toward Cys. This will be a sufficient way for design and development of Cys sensors applicable in environmental science and life science with high sensitivity and selectivity.

4. Conclusion

In conclusion, a novel fluorescent sensor **A1** containing a maleimide group as the recognition site was developed. It is applicable for fluorescence turn-on detection of Cys in both DMF and DMF/H_2O (9:1, v/v) media. Addition of Cys to **A1** solution in DMF induced bright blue fluorescence and emission intensity enhancement by 320-fold while other amino acids including Hcy, GSH, Gly, Glu, Val, Tyr, Arg, Trp, Lys, His, Leu, Phe, Asp and Met did not bring about remarked change. Sensor **A1** responds to Cys in seconds by sharp enhancement in the fluorescence emission. Immediately after addition of Cys to sensor **A1** solution in DMF the fluorescence intensity increased by 170-fold and attained the maximum value in 5 min. The detection limit of sensor **A1** toward Cys is 4.7 nM in DMF. Quantitative determination of Cys concentration is available by fluorescence titration experiments on sensor **A1** in both DMF and partially aqueous (DMF/H_2O = 9:1, v/v) solution. Sensor **A1** responds to Cys in DMF/H_2O (9:1, v/v) solution with a response time of

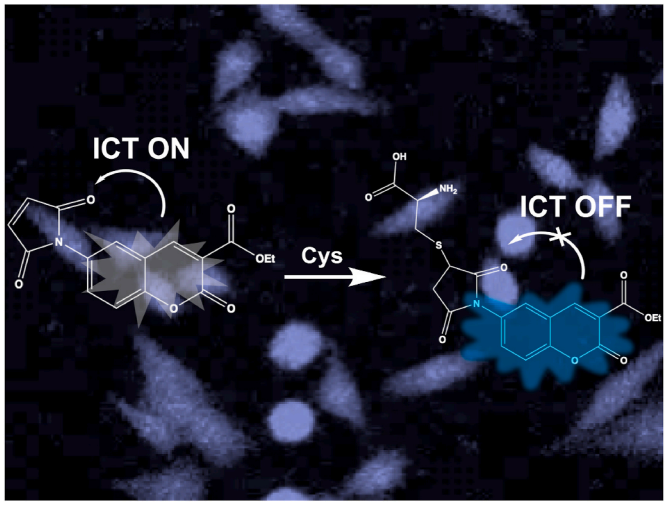

Scheme 3. Plausible sensing mechanism of sensor **A1** towards Cys.

7 min and the detection limit of 14 nM. Utilization of sensor **A1** to quantitative determination of Cys content in drugs and bioimaging of living Hela cells has been successfully performed. Possible sensing mechanism of sensor **A1** toward Cys has been proposed. Thus the study may throw a light on the reasonable development of efficient chemosensors for ultrasensitive and highly selective fluorescence turn-on discrimination of Cys from Hcy and GSH in both organic and aqueous media.

Authors' contributions

Conceiving and designing of the experiments: Y.Song, H.Li and Y. Sun; Performing research and analyzing the data: L.Hu, T.Zheng, J.Fan and R.Zhang; Writing of the paper: L.Hu, T.Zheng and H.Li.

All authors read and approved the final manuscript.

Appendix A. Supplementary data

Supplementary data to this article can be found online at https://doi.org/10.1016/j.ab.2021.114138.

References

[1] A. Pastore, A. Alisi, G. di Giovamberardino, A. Crudele, S. Ceccarelli, N. Panera, C. Dionisi-Vici, V. Nobili, Plasma levels of homocysteine and cysteine increased in pediatric NAFLD and strongly correlated with severity of liver damage, Int. J. Mol. Sci. 15 (2014) 21202–21214.

[2] S. Persichilli, J. Gervasoni, A. Di Napoli, A. Fuso, V. Nicolia, B. Giardina, S. Scarpa, C. Desiderio, R.A. Cavallaro, Plasma thiols levels in Alzheimer's disease mice under diet-induced hyperhomocysteinemia: effect of S-adeno-sylmethionine and superoxide-dismutase supplementation, J. Alzheimers Dis. 44 (2015) 1323–1331.

[3] S.A. Lipton, Y.-B. Choi, H. Takahashi, D. Zhang, W. Li, A. Godzik, L.A. Bankston, Cysteine regulation of protein function–as exemplified by NMDA- receptor modulation, Trends Neurosci. 25 (2002) 474–480.

[4] X.F. Wang, M.S. Cynader, Pyruvate released by astrocytes protects neurons from copper-catalyzed cysteine neurotoxicity, J. Neurosci. 21 (2001) 3322–3331.

[5] P.-Y. Chu, M.-Y. Liu, Amino acid cysteine induces senescence and decelerates cell growth in melanoma, J. Funct. Foods 18 (2015) 455–462.

[6] L.-Y. Niu, Y.-Z. Chen, H.-R. Zheng, L.-Z. Wu, C.-H. Tung, Q.-Z. Yang, Design strategies of fluorescent probes for selective detection among biothiols, Chem. Soc. Rev. 44 (2015) 6143–6160.

[7] Z. Xu, T. Qin, X. Zhou, L. Wang, B. Liu, Fluorescent probes with multiple channels for simultaneous detection of Cys, Hcy, GSH, and H_2S, Trends Anal. Chem. 121 (2019) 115672.

[8] Y. Yang, T. Zhou, M. Jin, K. Zhou, D. Liu, X. Li, F. Huo, W. Li, C. Yin, Thiol-chromene "click" reaction triggered self-immolative for NIR visualization of thiol flux in physiology and pathology of living cells and mice, J. Am. Chem. Soc. 142 (2020) 1614–1620.

[9] X. Xie, Z. Peng, X. Hua, Z. Wang, K. Deng, X. Yang, H. Huang, Selectively monitoring glutathione in human serum and growth-associated living cells using gold nanoclusters, Biosens. Bioelectron. 148 (2020) 111829.

[10] T. Jin, Y. Li, W. Jing, Y. Li, L. Fan, X. Li, Cobalt-based metal organic frameworks: a highly active oxidase-mimicking nanozyme for fluorescence "turn-on" assays of biothiol, Chem. Commun. 56 (2020) 659–662.

[11] A.S.K. Kumar, W.-B. Tseng, M.-J. Wu, Y.-Y. Huang, W.-L. Tseng, L-cystine- linked BODIPY-adsorbed monolayer MoS_2 quantum dots for ratiometric fluorescent sensing of biothiols based on the inner filter effect, Anal. Chim. Acta 1113 (2020) 43–51.

[12] J. Cao, X. Jiang, N. Fu, A sensitive fluorescent probe for imaging biothiol in zebrafish, Dyes Pigments 174 (2020) 107978.

[13] J. Dai, C. Ma, P. Zhang, Y. Fu, B. Shen, Recent progress in the development of fluorescent probes for detection of biothiols, Dyes Pigments 177 (2020) 108321.

[14] J. Zhang, N. Wang, X. Ji, Y. Tao, J. Wang, W. Zhao, BODIPY-based fluorescent probes for biothiols, Chem. Eur J. 26 (2020) 4172–4192.

[15] N. Zhou, Y. Shi, C. Sun, X. Zhang, W. Zhao, Carbon quantum dot-AgOH colloid fluorescent probe for selective detection of biothiols based on the inner filter effect, Spectrochim. Acta 228 (2020) 117847.

[16] J. Bai, X. Yang, Y. Qian, A ratiometric and near-infrared fluorescent probe for discrimination of Cys/Hcy/GSH in aqueous solution and its intracellular imaging in living cells, J. Lumin. 221 (2020) 117055.

[17] X. Song, Y. Yang, J. Ru, Y. Wang, F. Qiu, Y. Feng, G. Zhang, W. Liu, Highly specific monitoring and imaging of endogenous and exogenous cysteine in living cells, Talanta 204 (2019) 561–568.

[18] J. Li, Y. Yue, F. Huo, C. Yin, Rational design of cysteine-specific ratiometric probe based on steric hindrance effect and its biological application, Dyes Pigments 164 (2019) 335–340.

[19] P. Bhattacharjee, S. Chatterjee, A. Achari, A. Saha, D. Nandi, C. Acharya, K. Chatterjee, S. Ghosh, S. Swarnakar, P. Jaisankar, A bis-indole/carbazole based C5-curcuminoid fluorescent probe with large Stokes shift for selective detection of biothiols and application to live cell imaging, Analyst 145 (2020) 1184–1189.

[20] S. Wu, Y. Li, T. Deng, X. Wang, S. Hu, G. Peng, X. Huang, Y. Ling, F. Liu, A new fluorescent probe for sensing of biothiols and screening of acetylcholinesterase inhibitors, Org. Biomol. Chem. 18 (2020) 2468–2474.

[21] Y. Dang, L. Chen, L. Yuan, J. Li, D. Chen, A new fluorescent probe for selective detection of endogenous cysteine and live cell imaging, ChemistrySelect 5 (2020) 584–590.

[22] Q. Wang, X. Wei, C. Li, Y. Xie, A novel p-aminophenylthio- and cyano- substituted BODIPY as a fluorescence turn-on probe for distinguishing cysteine and homocysteine from glutathione, Dyes Pigments 148 (2018) 212–218.

[23] J.-Y. Xie, C.-Y. Li, Y.-F. Li, J. Fei, F. Xu, J. Ou-Yang, J. Liu, Near-infrared fluorescent probe with high quantum yield and its application in the selective detection of glutathione in living cells and tissues, Anal. Chem. 88 (2016) 9746–9752.

[24] Z.-w. Ning, S.-z. Wu, G.-j. Liu, Y.-m. Ji, L.-y. Jia, X.-x. Niu, R.-f. Ma, Y. Zhang, G.-w. Xing, Water-soluble AIE-active fluorescent organic nanoparticles: design, preparation and application for specific detection of cysteine over homocysteine and glutathione in living cells, Chem. Asian J. 14 (2019) 2220–2224.

[25] X. Dai, Q.-H. Wu, P.-C. Wang, J. Tian, Y. Xu, S.-Q. Wang, J.-Y. Miao, B.-X. Zhao, A simple and effective coumarin-based fluorescent probe for cysteine, Biosens. Bioelectron. 59 (2014) 35–39.

[26] X. Dai, T. Zhang, Y.-Z. Liu, T. Yan, Y. Li, J.-Y. Miao, B.-X. Zhao, A ratiometric fluorescent probe for cysteine and its application in living cells, Sens. Actuators, B 207 (2015) 872–877.

[27] Z.-H. Fu, X. Han, Y. Shao, J. Fang, Z.-H. Zhang, Y.-W. Wang, Y. Peng, Fluorescein-based chromogenic and ratiometric fluorescence probe for highly selective detection of cysteine and its application in bioimaging, Anal. Chem. 89 (2017) 1937–1944.

[28] S.J. Li, Y.J. Fu, C.Y. Li, Y.F. Li, J. OuYang, A near-infrared fluorescent probe based on BODIPY derivative with high quantum yield for selective detection of exogenous and endogenous cysteine in biological samples, Anal. Chim. Acta 994 (2017) 73–81.

[29] S. Feng, Y. Fang, W. Feng, Q. Xia, G. Feng, A colorimetric and ratiometric fluorescent probe with enhanced near-infrared fluorescence for selective detection of cysteine and its application in living cells, Dyes Pigments 146 (2017) 103–111.

[30] R.-F. Zeng, J.-S. Lan, X.-D. Li, H.-F. Liang, Y. Liao, Y.-J. Lu, T. Zhang, Y. Ding, A fluorescent coumarin-based probe for the fast detection of cysteine with live cell application, Molecules 22 (2017) 1618.

[31] Y. Wu, Y. Zhang, L. Wang, Y. Huyan, H. Li, Z. Pei, Y. Tang, S. Sun, Y. Xu, A simple ratiometric fluorescent sensor selectively compatible of different combinations of characteristic groups for identification of glutathione, cysteine and homocysteine, Sens. Actuators, B 302 (2020) 127181.

[32] X. Pei, F. Huo, Y. Yue, T. Chen, C. Yin, Cancer cell recognition by a Cys-reactive turn-on significant enhanced fluorescent emission targeting biotin receptors, Sens. Actuators, B 304 (2020) 127431.

[33] B. Zhang, H. Zhang, M. Zhong, S. Wang, Q. Xu, D.-H. Cho, H. Qiu, A novel off-on fluorescent probe for specific detection and imaging of cysteine in live cells and in vivo, Chin, Chem. Lett. 31 (2020) 133–135.

[34] M. Yoshida, M. Kamiya, T. Yamasoba, Y. Urano, A highly sensitive, cell-membrane-permeable fluorescent probe for glutathione, Bioorg. Med. Chem. Lett 24 (2014) 4363–4366.

[35] G.-J. Kim, D.-H. Yoon, M.-Y. Yun, H. Kwon, H.-J. Ha, H.-J. Kim, An activatable fluorescent probe for targeting cellular membrane through the biothiol-mediated hydrazone-to-pyrazole transformation, Sens. Actuators, B 211 (2015) 245–249.

[36] C. Wang, Y. Wang, G. Wang, S. Chen, C. Huang, Two-isophorone fluorophore-based design of a ratiometric fluorescent probe and its application in the sensing of biothiols, J. Mater. Chem. B 7 (2019) 5633–5639.

[37] X. Lin, Y. Hu, D. Yang, B. Chen, Cyanine-coumarin composite NIR dye based instantaneous-response probe for biothiols detection and oxidative stress assessment of mitochondria, Dyes Pigments 174 (2020) 107956.

[38] A. Ren, D. Zhu, Y. Luo, A novel Boranil-based turn-on fluorescent probe for imaging of biothiols in living cells, J. Mol. Struct. 1209 (2020) 127914.

[39] D. Jung, S. Maiti, J.H. Lee, J.H. Lee, J.S. Kim, Rational design of biotin- disulfide-coumarin conjugates: a cancer targeted thiol probe and bioimaging, Chem. Commun. 50 (2014) 3044–3047.

[40] S.-R. Liu, C.-Y. Chang, S.-P. Wu, A fluorescence turn-on probe for cysteine and homocysteine based on thiol-triggered benzothiazolidine ring formation, Anal. Chim. Acta 849 (2014) 64–69.

[41] X. Chen, Y. Zhou, X. Peng, J. Yoon, Fluorescent and colorimetric probes for detection of thiols, Chem. Soc. Rev. 39 (2010) 2120–2135.

[42] S.V. Mulay, Y. Kim, M. Choi, D.Y. Lee, J. Choi, Y. Lee, S. Jon, D.G. Churchill, Enhanced doubly activated dual emission fluorescent probes for selective imaging of glutathione or cysteine in living systems, Anal. Chem. 90 (2018) 2648–2654.

[43] L. He, X. Yang, K. Xu, W. Lin, Improved aromatic substitution– rearrangement-based ratiometric fluorescent cysteine-specific probe and its application of real-time imaging under oxidative stress in living zebrafish, Anal. Chem. 89 (2017) 9567–9573.

[44] Y. Zou, M. Li, Y. Xing, T. Duan, X. Zhou, F. Yu, Bioimaging of glutathione with a two-photon fluorescent probe and its potential application for surgery guide in laryngeal cancer, ACS Sens. 5 (2020) 242–249.

[45] K.-B. Li, W.-B. Qu, Q. Shen, S. Zhang, W. Shi, L. Dong, D.-M. Han, 1,8-Naphthalimide-based dual-response fluorescent probe for highly discriminating detection of cys and H_2S, Dyes Pigments 173 (2020) 107918.

[46] H. Li, X. Sun, T. Zheng, Z. Xu, Y. Song, X. Gu, Coumarin-based multifunctional chemosensor for arginine/lysine and Cu^{2+}/Al^{3+} ions and its Cu^{2+} complex as

colorimetric and fluorescent sensor for biothiols, Sens. Actuators, B 279 (2019) 400–409.
[47] J.P. Lee, F. Jannah, K. Bae, J.-M. Kim, A colorimetric and fluorometric polydiacetylene biothiol sensor based on decomposition of a pyridine-mercury complex, Sens. Actuators, B 309 (2020) 127771.
[48] X. Pang, J. Dong, L. Gao, L. Wang, S. Yu, J. Kong, L. Li, Dansyl-peptide dual-functional fluorescent chemosensor for Hg^{2+} and biothiols, Dyes Pigments 173 (2020) 107888.
[49] P.P.P. Kumar, N. Kaur, A. Shanavas, P.P. Neelakandan, Nanomolar detection of biothiols via turn-ON fluorescent indicator displacement, Analyst 145 (2020) 851–857.
[50] X. Li, J. Qiao, Z. Li, L. Qi, Fluorescence turn-off-on for highly selective detection of serum L-cysteine based on AuNCs-AuNPs ensembles, Analyst 145 (2020) 2233–2237.
[51] T.O. Sippel, New fluorochromes for thiols: maleimide and iodoacetamide derivatives of a 3-phenylcoumarin fluorophore, J. Histochem. Cytochem. 29 (1981) 314–316.
[52] T.O. Sippel, Microfluorometric analysis of protein thiol groups with a coumarinylphenylmaleimide, J. Histochem. Cytochem. 29 (1981) 1377–1381.
[53] Y. Yang, F. Huo, C. Yin, J. Chao, Y. Zhang, An 'OFF-ON' fluorescent probe for specially recognize on Cys and its application in bioimaging, Dyes Pigments 114 (2015) 105–109.
[54] Y. Liu, Y. Liu, W. Liu, S. Liang, Two-photon fluorescent probe derived from naphthalimide for cysteine detection and imaging in living cells, Spectrochim, Acta 137 (2015) 509–515.
[55] T. Liu, F. Huo, J. Li, J. Chao, Y. Zhang, C. Yin, A fast response and high sensitivity thiol fluorescent probe in living cells, Sens. Actuators, B 232 (2016) 619–624.
[56] X. Li, Y. Zheng, H. Tong, R. Qian, L. Zhou, G. Liu, Y. Tang, H. Li, K. Lou, W. Wang, Rational design of an ultrasensitive and highly selective chemodosimeter by a dual quenching mechanism for cysteine based on a facile michael- transcyclization cascade reaction, Chem. Eur J. 22 (2016) 9247–9256.
[57] Z. Chen, Q. Sun, Y. Yao, X. Fan, W. Zhang, J. Qian, Highly sensitive detection of cysteine over glutathione and homo-cysteine: new insight into the Michael addition of mercapto group to maleimide, Biosens. Bioelectron. 91 (2017) 553–559.
[58] J. Qian, G. Zhang, J. Cui, L. Zhou, Z. Chen, Z. Zhang, W. Zhang, Fluorescent detection of biothiols with maleimide-based probes: effect of the spacer on the selectivity, Sens. Actuators, B 311 (2020) 127923.
[59] X. Gao, Y. Song, Q. Zhang, X. Liu, L. Tang, J. Li, Application of maleimide modified graphene quantum dots and porphyrin fluorescence resonance energy transfer in the design of "turn-on" fluorescence sensors for biothiols, Anal. Chim. Acta 1108 (2020) 46–53.
[60] F. Dong, H. Lai, Y. Liu, Q. Li, H. Chen, S. Ji, J. Zhang, Y. Huo, Highly selective isomer fluorescent probes for distinguishing homo-/cysteine from glutathione based on AIE, Talanta 206 (2020) 120177.
[61] P. Tao, D. Chen, Z. Xu, Y. Song, H. Li, C. Xian, A fluorescent probe for the dual detection of mercury ions and thiols based on a simple coumarin derivative, Color. Technol. 136 (2020) 75–86.
[62] D. Cao, Z. Liu, P. Verwilst, S. Koo, P. Jangjili, J.S. Kim, W. Lin, Coumarin-based small-molecule fluorescent chemosensors, Chem. Rev. 119 (2019) 10403–10519.
[63] X.-y. Sun, T. Liu, J. Sun, X.-j. Wang, Synthesis and application of coumarin fluorescence probes, RSC Adv. 10 (2020) 10826–10847.
[64] H.K. Chaudhari, A. Pahelkar, B.S. Takale, Preparative-scale synthesis of amino coumarins through new sequential nitration and reduction protocol, Tetrahedron Lett. 58 (2017) 4107–4110.
[65] G.-x. Yin, T.-t. Niu, Y.-b. Gan, T. Yu, P. Yin, H.-m. Chen, Y.-y. Zhang, H.-t. Li, S.-z. Yao, A multi-signal fluorescent probe with multiple binding sites for simultaneous sensing of cysteine, homocysteine, and glutathione, Angew. Chem. Int. Ed. 57 (2018) 4991–4994.
[66] Y.-F. Kang, H.-X. Qiao, Y.-L. Meng, Z.-H. Xin, L.-P. Ge, J.-N. Zheng, Y.-N. Wang, A simple and sensitive fluorescent probe for specific detection of cysteine, J. Chem. Sci. 129 (2017) 1219–1223.
[67] Y.-F. Kang, H.-X. Qiao, Y.-L. Meng, Z.-H. Xin, L.-P. Ge, M.-Y. Dai, J.-J. Xu, C.-H. Zhang, Selective detection of cysteine over homocysteine and glutathione by a simple and effective probe, Anal. Methods 9 (2017) 1707–1709.
[68] Z. Ye, C. Duan, Q. Hu, Y. Zhang, C. Qin, L. Zeng, A dual-channel responsive near-infrared fluorescent probe for multicolour imaging of cysteine in living cells, J. Mater. Chem. B 5 (2017) 3600–3606.
[69] J. Liu, Y.-Q. Sun, H. Zhang, Y. Huo, Y. Shi, H. Shi, W. Guo, A carboxylic acid-functionalized coumarin-hemicyanine fluorescent dye and its application to construct a fluorescent probe for selective detection of cysteine over homocysteine and glutathione, RSC Adv. 4 (2014) 64542–64550.
[70] L. Yan, Z. Kong, W. Shen, W. Du, Y. Zhou, Z. Qi, A label-free turn-on fluorescence probe for rapidly distinguishing cysteine over glutathione in water solution, Anal. Biochem. 500 (2016) 1–5.
[71] X. Zhou, X. Jin, G. Sun, X. Wu, A sensitive and selective fluorescent probe for cysteine based on a new response-assisted electrostatic attraction strategy: the role of spatial charge configuration, Chem. Eur J. 19 (2013) 7817–7824.
[72] Y. Yang, H. Wang, Y.-L. Wei, J. Zhou, J.-F. Zhang, Y. Zhou, A selective coumarin-based "turn-on" fluorescent sensor for the detection of cysteine and its applications for bioimaging, Chin. Chem. Lett. 28 (2017) 2023–2026.
[73] H. Tong, J. Zhao, X. Li, Y. Zhang, S. Ma, K. Lou, W. Wang, Orchestration of dual cyclization processes and dual quenching mechanisms for enhanced selectivity and drastic fluorescence turn-on detection of cysteine, Chem. Commun. 53 (2017) 3583–3586.